



Halogen Bonding in the Molecular Recognition of Thyroid Hormones and Their Metabolites by Transport Proteins and Thyroid Hormone Receptors

Santanu Mondal^{1,2}, Debasish Giri¹ and Govindasamy Mugesh^{1*}

Abstract | Halogen bonding (XB) is an attractive interaction between a halogen atom and an electron donor. Although halogens are electron-rich atoms, they act as electrophiles in these types of interactions. This is due to the presence of a significant positive charge (σ -hole) on the halogen atoms in organic halides along the R-X (R = carbon, nitrogen, halogen) bond. With an increase in the polarizability down the group from fluorine to iodine, the positive charge on the σ -hole increases, which leads to an increase in the strength of XB. Numerous studies revealed that XB is a useful tool to develop supramolecular architectures by self-assembly. Interestingly, XBs are also observed in many biomolecules, such as protein–ligand complexes and nucleic acids containing halogenated nucleotides. In fact, XBs are extensively used to increase the potency and selectivity of small molecule ligands to a target protein. In this minireview, we discuss the role of XBs in the molecular recognition of thyroid hormones (THs) and their metabolites by various transport proteins and thyroid hormone receptors (TRs). THs are naturally occurring iodinated small molecules that are synthesized by the thyroid gland and carried to various target organs by several serum transport proteins, such as transthyretin, human serum albumin, and thyroxine-binding globulin. Interestingly, all these proteins form XBs with THs and these interactions play important roles in the high affinity binding. Furthermore, TRs, such as TR α and TR β also form XBs with the 3-iodine of THs and triiodothyroacetic acid, an endogenous TH metabolite that shows thyromimetic activity.

Keywords: Halogen bond, Thyroid hormones, Thyroid hormone receptors, Transport proteins

1 Introduction

Group 17 elements of the Periodic Table or halogens are typically known as highly electronegative elements. In most cases, halogens function as electron donor sites (nucleophile) in many noncovalent interactions, including hydrogen bonding and in forming coordinate bond with alkali- and alkaline-earth metal ions.^{1–3} However,

over the last century, halogens, particularly the heavier ones, have increasingly been recognized as electrophilic sites (Lewis acid). In such scenario, they form charge-transfer interactions in the presence of an electron donor (Lewis base). Such type of charge-transfer interactions was known since 1814 when J. J. Colin reported the reaction of dry iodine with dry gaseous

¹ Department of Inorganic and Physical Chemistry, Indian Institute of Science, Bangalore 560012, India.

² Department of Biochemistry and Molecular Pharmacology, University of Massachusetts Medical School, Worcester, MA 01605, USA.

*mugesh@iisc.ac.in

ammonia to afford a liquid with $I_2 \cdots NH_3$ interactions.⁴ Five years later, in 1819, P. Pelletier and J. B. Caventou reported the synthesis of strychnine triiodide, where the triiodide anion (I_3^-) is formed by the attractive interaction of iodine with iodide.⁵ Based on the overwhelming subsequent reports on the formation of such charge-transfer interactions, in 2009, International Union of Pure and Applied Chemistry (IUPAC) started a project (project no. 2009-032-1-100) to take a comprehensive look at intermolecular interactions involving halogens as electrophilic species and classify them.⁶ In 2013, these interactions received an IUPAC recommendation as halogen bonds.⁷ Therefore, halogen bond (XB) is generally described as the noncovalent interaction, $D \cdots X-R$, where X is an electrophilic halogen (XB donor), D is a donor of electron density (XB acceptor), and R is a carbon, nitrogen, or halogen atom (Fig. 1a).

The electrophilic nature of halogens in organic halide originates from the anisotropic charge distribution. Many theoretical as well as experimental studies have shown that covalently bonded halogen atoms contain a significant amount of positive potential along the R-X (Fig. 1a) axis, and this region is called as σ -hole.^{8,9} Notably, as the polarizability increases down the group from F to I, the positive charge on σ -hole increases. As shown in Fig. 1b, the electrostatic potential remains negative around the fluorine atom in CH_3F , while a region of positive potential emerges for chlorine, bromine,

and iodine atoms in CH_3Cl , CH_3Br , and CH_3I , respectively.¹⁰ In contrast, electrostatic potential remains neutral all around methane (Fig. 1b). Furthermore, σ -hole is surrounded by an electro-neutral ring and further out, a negatively charged belt. Therefore, halogens can act as electrophile on approaching along the R-X axis (pole), whereas they behave as nucleophile on approaching perpendicular to the R-X axis (equator). As σ -hole is responsible for the formation of XBs, the strength of XB increases in the order $F < Cl < Br < I$ and often times, this trend is used to characterize XBs. Notably, the strength of XBs can be enhanced by introducing electron-withdrawing groups on the carbon skeleton attached to the halogen atom.¹¹ Similarly, an increase in the electronegativity of the atom/moiety directly attached to halogen atom results in the formation of stronger XB, and therefore, XB strength order of $C(sp)-X > C(sp^2)-X > C(sp^3)-X$ is generally followed.¹²⁻¹⁴ The strength of XB is evaluated by the $D \cdots X$ interatomic distance—shorter the distance, stronger the interaction. Consistent with the electron donation from the XB acceptor to the antibonding orbital of the R-X bond, the formation of XB leads to a lengthening of the R-X bond.¹⁵ XBs have extensively been used to form supramolecular architectures via self-assembly, to bind anions in solid and solution states, to catalyse organic transformations, to tune the photophysical emissive properties of organic chromophores, to resolve enantiomers, and to tailor the magnetic and conductive properties of

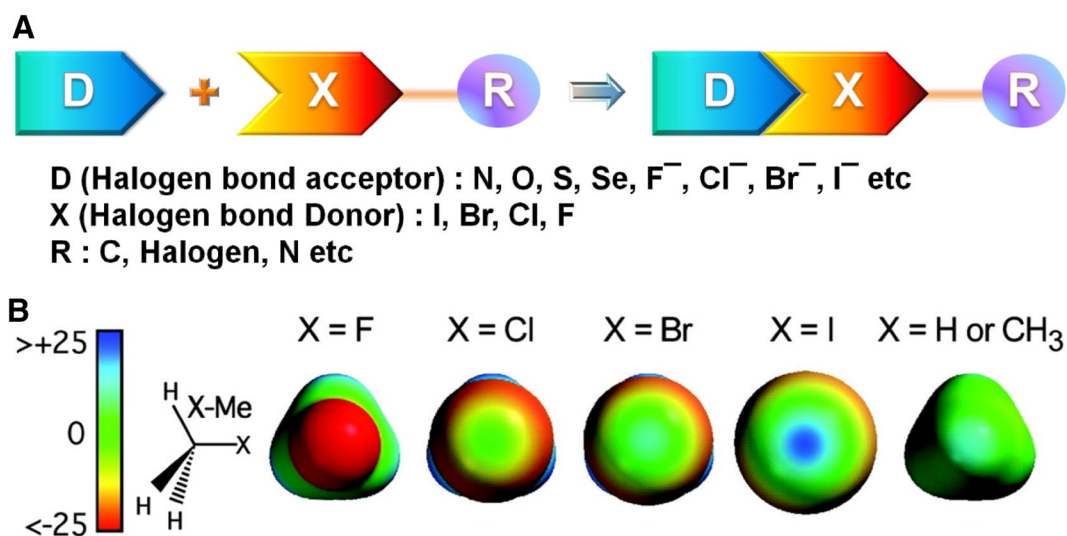


Figure 1: a Schematic representation of halogen bond. b *Ab initio* electrostatic potential surfaces of halogenated methanes (X-Me) and methane (last column), indicating the negative (red), neutral (green), and positive (blue) electrostatic potentials around the halogen surfaces. Reproduced from reference 10 with permission.¹⁰

molecular materials, and all these aspects have been discussed in several excellent reviews.^{16–19}

Halogen bonding has also been found in several protein–ligand complexes as well as nucleic acids containing halogenated nucleotides.^{10, 20–25} Notably, incorporation of halogen has been a useful tool in medicinal chemistry to increase the potency and selectivity of bioactive small molecules to a target protein.^{23–26} Additionally, Mugesh and coworkers have recently shown that incorporation of halogens in small molecule fluorophores as well as fluorescent proteins, such as green fluorescent protein (GFP), dramatically enhances their cellular uptake, possibly due to the formation of XBs with cell surface receptors.^{27–29} In protein–ligand complexes, XBs are formed between the halogenated ligand and a properly oriented electron donor (Lewis base) in the binding pocket. Backbone carbonyl functionality (C=O) in the amino acids has been found to be the most frequent Lewis base involved in the formation of XBs in protein–ligand complexes. However, the side chain functionalities, such as hydroxyls in Ser, Thr and Tyr, sulphurs in Cys and Met, carboxylates in Asp and Glu, imidazole nitrogens in His, and the aromatic π -systems in Phe, Tyr, Trp, and His can also form XBs.^{10, 24, 25, 30} In this minireview, we focus on the role of XBs in the molecular recognition of thyroid hormones (THs) and their metabolites, which are probably the best known examples of naturally occurring iodinated molecules that bind to various transport proteins and thyroid hormone receptors.

2 Thyroid Hormones and Their Action

Thyroid hormones are key players of human endocrine system and they control almost every processes in the body, including brain development, growth, carbohydrate and fat metabolism, protein synthesis, and cardiovascular and renal functions. Thyroid hormones are biosynthesized in the follicular lumen of the thyroid gland, and their secretion is controlled by the hypothalamus and pituitary gland in brain.^{31–34} With help of iodide (imported by sodium iodide symporter) and hydrogen peroxide (generated by dual oxidases), thyroid peroxidase (TPO) iodinates tyrosine residues in thyroglobulin (Tg), a tyrosine-rich glycoprotein on which thyroxine biosynthesis takes place, and this process is known as organification of inorganic iodide. Phenolic coupling of two diiodotyrosine residues on Tg (catalysed by thyroid peroxidase) and subsequent proteolysis release the prohormone, 3,5,3',5'-tetraiodothyronine (thyroxine or T4) into blood stream (Fig. 2, 3a).³⁵ T4 is then carried into various target organs by three transport proteins in serum—thyroxine-binding globulin (TBG), transthyretin (TTR), and serum albumin (HSA, for human).³⁶ In the target organs, the prohormone is then converted to the biologically active metabolite, 3,5,3'-triiodothyronine (T3, Fig. 3a) by regioselective phenolic ring (5') deiodination, catalysed by mammalian selenoenzymes, and iodothyronine deiodinase type 1 (DIO1) and type 2 (DIO2).^{37–40} Subsequently, T3 binds to the nuclear thyroid hormone receptors (TRs)

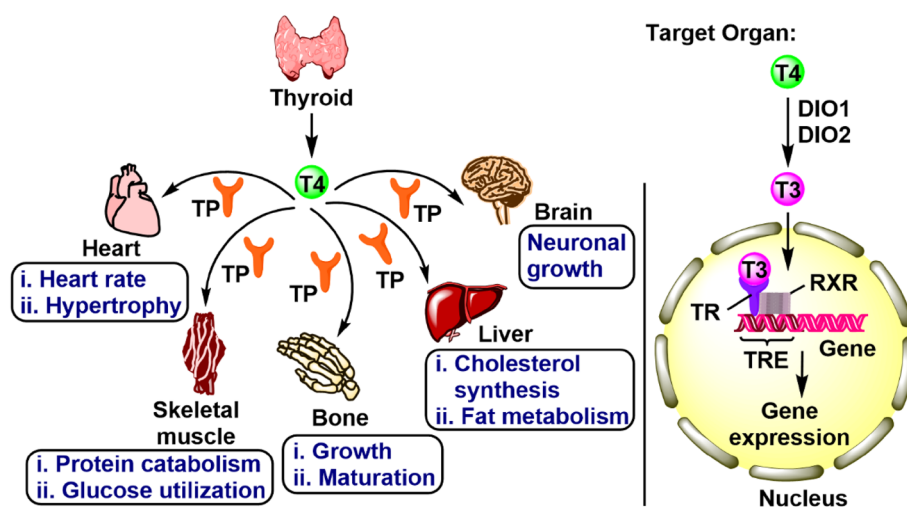


Figure 2: Schematic representation of secretion, transport, and action of thyroid hormones, T4 and T3 in the target organs. TP: transport protein, DIO: iodothyronine deiodinase, TR: thyroid hormone receptor, TRE: thyroid hormone responsive element, RXR: retinoid X receptor.

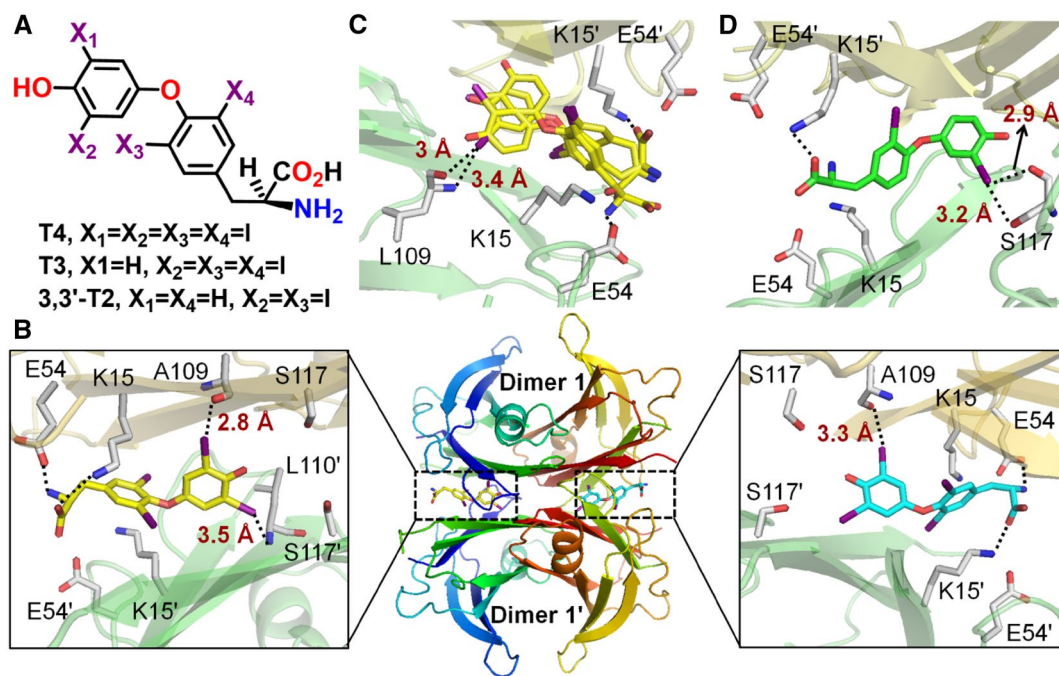


Figure 3: **a** Chemical structures of T4, T3, and 3,3'-T2. **b** X-ray crystal structure of human transthyretin (TTR) bound to T4, indicating the hydrogen and halogen-bonding interactions responsible for T4-binding (PDB code: 2ROX).⁴⁴ X-ray crystal structure of sea bream (C), (PDB code: 1SN5)⁴⁵ and human (D), (PDB code: 1THA)⁴⁶ TTR in complex with T3 and 3,3'-T2, respectively, indicating the interactions responsible for molecular recognition.

that exist as homodimer or heterodimer with the 9-cis-retinoic acid receptor (RXR). The binding of TR/RXR complex to the thyroid hormone responsive elements (TREs, a specific nucleotide sequence) on the target genes facilitates the activation of co-repressor and co-activator proteins that ultimately regulate gene expression (Fig. 2).^{41, 42} Interestingly, both T4 and T3 form XB with the transport proteins as well as nuclear receptors, and these interactions play important roles in the molecular recognition process. Furthermore, several biochemical and biomimetic studies suggest that the selenocysteine in the active site of DIOs form XB with THs to polarize the C–I bond for reductive deiodination. In the following sections, we discuss the XBs formed by THs and their metabolites with transport proteins and nuclear thyroid hormone receptors.

3 Thyroid Hormone Transport Proteins

Owing to high hydrophobicity, THs cannot circulate in the blood in the free (unbound) state. As soon as they enter the blood stream from the thyroid gland, three transport proteins, TBG, TTR, and HSA bind them, and carry to various

target organs.^{35, 36} Although TBG exhibits the highest affinity for THs amongst the three proteins, higher plasma concentrations of TTR (4.6 μ M) and HSA (640 μ M) compared to TBG (0.27 μ M) make TTR and HSA as high-capacity TH carrier.³⁶ Owing to low affinity, the binding of THs to TTR and HSA exhibits fast dissociation kinetics. Notably, the dissociation of T4 from the ligand-binding sites facilitates the unfolding of TTR, leading to the formation of toxic amyloid aggregates and their deposition in various organs.⁴³ Almost 74% of total T4 is carried by TBG, while only 11% and 15% of the same remain bound to TTR and HSA, respectively. However, TTR is the only TH-binding protein in the cerebrospinal fluid (CSF).³⁵ Binding of THs to serum transport proteins also ensure the slow clearance and prolonged half-life in blood serum.

4 Transthyretin (TTR)

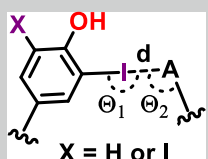
Although TBG is the major TH carrier in serum in humans, in rat and other lower vertebrates, TTR is the primary TH carrier. TTR (also known as prealbumin) is mainly synthesized in liver. TTR also transports Vitamin A by forming a stable complex with retinol-binding protein (RBP)

at the outer surface.^{35, 36} Although TTR exhibits the highest affinity (100%) for binding T4, it can also bind various TH metabolites with lower iodine content, such as T3, 3,3'-T2 and 3-T1 (Fig. 3a). However, the affinity of TTR for these metabolites is remarkably lower (0.07% for 3,3'-T2, <0.01% for 3-T1) than that observed for T4, indicating that the number of iodine atoms also plays an important role in the binding.^{35, 36} TTR exhibits a homotetrameric quaternary structure with a molecular weight of 55 kDa and this structure results from the assembly of four identical 127 residue polypeptide chains or monomers (A, B, C, and D) around a central channel (Fig. 3b).⁴⁴ Each monomer unit has a β -barrel structure consisting of eight strands (A–H) and a short α -helix after F strand. Although TTR contains two sterically equivalent T4-binding sites (Site I and II) at the weak dimer–dimer interface (Fig. 3b), these sites exhibit different binding affinity for T4. Site I (between monomer A and C) exhibits 100-times higher affinity for T4 than site II (between monomer B and D) (dissociation constant (K_d), 10^{-8} M for site I and 10^{-6} M for site II) and a negative cooperative effect for the binding of T4 to TTR is proposed.^{35, 36}

The crystal structure of human TTR–T4 complex (orthorhombic form, PDB code: 2ROX) indicates that in both site I and II, the 4'-OH group of T4 points towards the centre of the channel, while the β -alanine side chain protrudes towards the solvent-exposed surface. This binding orientation is called as the forward mode, while the opposite orientation with 4'-OH group towards the surface and β -alanine side chain towards the central channel is called as reverse mode. In the forward mode, 4'-OH group is stabilized by hydrogen bonding with S117, while the β -alanine side chain forms salt-bridge interactions with K15 and E54 residues (Fig. 3b).⁴⁴ TTR also contains three pairs of symmetry-related halogen-binding pockets (HBPs), HBP1(HBP1'), HBP2(HBP2'), HBP3(HBP3') comprising the hydrophobic side chains and nucleophilic backbone carbonyl groups. For example, HBP3 is formed by backbone and side chains of A108, A109, L110, T188, T119, and S11. Interestingly, in site I, the 3- and 5-iodine atoms are accommodated in HBP1 and HBP1' pockets through hydrophobic interactions, while the 3'-iodine in HBP3' forms a strong I...O XB with the backbone carbonyl of A109 (Fig. 3b, see left panel). This XB is characterized by an I...O distance (d) of 2.8 Å, which is 20% shorter than the sum of van der Waal's radii of oxygen and iodine (3.5 Å).⁴⁴ Furthermore, Θ_1 ($\angle C_{T4}IO$) and Θ_2 ($\angle IOC_{A109}$), as shown in

Table 1, are 162.0° and 94.1°, respectively, which are in agreement with the proposed ideal geometry ($\Theta_1 \sim 180^\circ$ and $\Theta_2 \sim 90^\circ$) for effective formation of XB.^{16, 18, 19} 3'-Iodine also forms a weak XB with the backbone NH of A109 with I...N distance of 3.5 Å (0.8% shorter than the sum of van der Waal's radii of iodine and nitrogen, 3.53 Å), and Θ_1 and Θ_2 of 134.7° and 93.5°, respectively (Fig. 3b and Table 1). Although Θ_1 for this interaction is deviated from the ideal geometry, significant numbers of XBs with Θ_1 between 130° and 150° are known in several protein–ligand complexes.^{10, 24} 5'-Iodine atom also form a weak I...N XB with the backbone NH of L110'. Generally, the amidic nitrogen atom forms weak halogen bond due to the conjugation of the lone pair of nitrogen atom with the carbonyl group. This XB is characterized by $d_{I...N}$, Θ_1 , and Θ_2 of 3.5 Å, 134.1°, and 100.9°, respectively. In contrast to site I, only one I...O XB ($d_{I...O}$: 3.3 Å, Θ_1 : 166.8°, Θ_2 : 90.4°) is observed between the 3'-iodine and backbone carbonyl of A109 in site II (Fig. 3b, see right panel and Table 1).⁴⁴ Notably, this I...O XB is weaker than that observed in site I. These observations indicate that the formation of weaker XB as well as fewer interactions may account for the 100-fold lower affinity of site II for T4 than site I.

The monoclinic form of human TTR in complex with T4 (PDB code: 1ICT) indicates extensive formation of XBs in both the sites involving the 3'- and 5'-iodine of T4.⁴⁷ In contrast to the orthorhombic form, 3'-iodine forms three moderately strong XBs with the backbone carbonyl of A108, and backbone NH of A109 and L110 residues (Table 1). The 5'-iodine forms two XBs with the backbone carbonyl and side chain hydroxyl group of S117' residue, although the XB formed with backbone carbonyl ($d_{I...O}$: 3.3 Å) is little stronger than with the side chain hydroxyl ($d_{I...O}$: 3.4 Å). In site II, T4 moves 1.5 Å deeper towards the central channel compared to Site I, thereby placing the 3'- and 5'-iodine atoms in HBP3 and HBP3' pockets. In site II, 3'-iodine forms only one XB with the backbone NH of T119 with a I...N distance of 3.3 Å (6.5% shorter than the sum of van der Waal's radii) (Table 1). Similar to site I, the other phenolic iodine atom (5') interacts with the backbone carbonyl and side chain hydroxyl group of S117', although, in contrast to site I, both these interactions are of equal strength ($d_{I...O}$: 3.2 Å, 8.6% shorter than the sum of van der Waal's radii). Additionally, 5'-iodine also forms a I...N XB with the backbone NH of T119' ($d_{I...N}$: 3.4 Å, Θ_1 : 115.1°, Θ_2 : 107.2°).⁴⁷

Table 1: XBs observed in the crystal structures of TTR in complex with various THs and metabolites.


PDB Code	TTR	Ligand (Iodine)	XB acceptor (A)	XB parameters		
				d (Å)	Θ_1 (°)	Θ_2 (°)
2ROX	Human	T4 (3')	A109 (backbone O, site I)	2.8	162.7	94.1
		T4 (3')	A109 (backbone NH, site I)	3.5	134.7	93.5
		T4 (5')	L110' (backbone NH, site I)	3.5	134.1	100.9
		T4 (3')	A109 (backbone O, site II)	3.3	166.8	90.4
1ICT	Human	T4 (3')	A108 (backbone O, site I)	3.2	149.3	72.3
		T4 (3')	A109 (backbone NH, site I)	3.1	135.5	81.8
		T4 (3')	L110 (backbone NH, site I)	3.2	114.0	118.3
		T4 (5')	S117' (backbone O, site I)	3.3	166.1	102.4
		T4 (5')	S117' (side chain O, site I)	3.4	132.7	108.1
		T4 (3')	T119 (backbone NH, site II)	3.3	144.5	113.0
		T4 (5')	S117' (backbone O, site II)	3.2	111.8	84.8
		T4 (5')	S117' (side chain O, site II)	3.2	104.6	96.5
1ETA	Human	T4 (3')	A109 (backbone O, site I)	3.1	149.4	106.1
		T4 (3')	A109 (backbone O, site II)	3.1	161.0	102.2
1ETB	Human	T4 (3')	T109 (backbone O, site I)	3.3	159.7	93.0
		T4 (3')	T109 (backbone O, site II)	3.2	161.2	91.8
1IE4	Rat	T4 (3')	A109 (backbone O, site I)	3.1	158.2	100.9
		T4 (3')	A109 (backbone O, site II)	3.4	132.2	77.6
		T4 (3')	A109 (backbone NH, site II)	3.4	151.1	91.8
		T4 (5')	A109' (backbone NH, site II)	3.5	113.5	88.9
1SNO	Sea bream	T4 (3')	L109 (backbone NH, site I)	3.5	131.7	109.7
		T4 (5')	L109' (backbone O, site I)	3.4	153.3	81.0
		T4 (3')	L109 (backbone O, site II)	3.3	162.3	87.3
		T4 (5')	L109' (backbone O, site II)	3.3	169.7	86.9
		T4 (5')	L109' (backbone NH, site II)	3.5	130.9	104.4
1SN5	Sea bream	T3 (3')	L109 (backbone O, site I)	3.0	172.6	96.4
		T3 (3')	L109 (backbone NH, site I)	3.4	129.3	106.2
1THA	Human	3,3'-T2 (3')	S117 (backbone O, site I)	3.4	134.9	86.8
		3,3'-T2 (3')	S117 (backbone O, site II)	3.2	144.8	84.2
		3,3'-T2 (3')	S117 (side chain O, site II)	2.9	102.5	128.7
1Z7J	Human	TA4 (3')	A109 (backbone O, site I)	2.8	164.0	95.6
		TA4 (3')	A109 (backbone NH, site I)	3.5	125.2	93.7
		TA4 (3')	A309 (backbone O, site II)	3.0	177.7	87.9
		TA4 (3')	L310 (backbone NH, site II)	3.5	138.7	80.3
1KGI	Rat	TA4 (3')	A309 (backbone O, site II)	3.1	159.5	103.3
		TA4 (3')	A709 (backbone O, site II)	3.1	154.2	102.5
		TA4 (3')	A709 (backbone NH, site II)	3.4	137.7	104.9

Another X-ray crystal structure of human TTR in complex with T4 (PDB code: 1ETA) at 1.7 Å resolution was solved by Hamilton et al.⁴⁸ In contrast to the orthorhombic form described earlier, this structure (also in the orthorhombic form) shows that in both the sites, 3'-iodine of T4 forms an equally strong I...O XB ($d_{I...O}$: 3.1 Å) with the backbone carbonyl of A109 (Table 1).⁴⁸ Authors have also solved the structure of an A109T variant of TTR, associated with euthyroid hyperthyroxinemia, in complex with T4 (PDB code: 1ETB).⁴⁹ Interestingly, this variant also forms I...O XBs with its T109 residue in both the sites. However, these XBs were found to be weaker ($d_{I...O}$: 3.3 Å in site I and 3.2 Å in site II, Table 1) than that observed in case of wild-type protein.

Rat TTR-T4 complex crystallizes in the tetragonal form (PDB code: 1IE4) and this crystal structure exhibits that in addition to hydrogen bonding and ion pair interactions in site I, the 3'-iodine forms a moderately strong I...O XB ($d_{I...O}$: 3.1 Å, Θ_1 : 158.2°, Θ_2 : 100.9°) with A109 residue.⁵⁰ In contrast, in site II, 3'-iodine forms both I...O and I...N XBs with the backbone carbonyl and NH groups of A109, respectively, while 5'-iodine forms only I...N (with A109') XB (Table 1). However, these XBs are found to be much weaker than that observed in site I.⁵⁰ In contrast to rat and human TTR, sea bream TTR in site I does not form any I...O XB with the 3'-iodine of T4.⁴⁵ However, a weak I...N XB ($d_{I...N}$: 3.5 Å, Θ_1 : 131.7°, Θ_2 : 109.7°, Table 1) is formed by backbone NH of L109 with the 3'-iodine of T4. In this site, a weak I...O interaction is also formed by the 5'-iodine of T4 with the backbone carbonyl of L109' residue. As shown in Table 1, relatively stronger XB interactions are formed in site II by both the 3'- and 5'-iodine atoms of T4 with L109 and L109' residues.⁴⁵ These observations indicate that human TTR forms much stronger XBs with T4 than rat or sea bream TTR, and it appears that TTR has evolved in higher vertebrates to bind T4 more efficiently.

TTR is also known to bind various metabolites of T4 and several crystal structures of TTR in complex with T4 metabolites have been reported in literature. Crystal structure of sea bream TTR-T3 complex (PDB code: 1SN5) reveals different binding modes for T4 and T3.⁴⁵ Interestingly, sea bream TTR exhibits higher affinity for T3 than T4, whereas human and rat TTR exhibit higher affinity for T4 than T3. The 3- and 5-iodine atoms of both T3 and T4 occupy the same halogen-binding pockets (HBP1 and HBP1'),

while the 3'-iodine atom of T3 occupies a place of that is occupied by the 4'-hydroxyl group of T4. In site I, three different binding modes for T3 were observed on the basis of electron density maps of 4'-hydroxyl group and 3'-iodine atom (Fig. 3c). In one of these modes, 3'-iodine forms a strong I...O ($d_{I...O}$: 3.0 Å, Θ_1 : 172.6°, Θ_2 : 96.4°) and a moderate I...N ($d_{I...N}$: 3.4 Å, Θ_1 : 129.3°, Θ_2 : 106.2°) XB with the backbone of L109 (Table 1).⁴⁵ Whereas in site II, none of these XBs are observed, indicating that site I may have higher affinity to T3 like T4. The formation of strong I...O XB with T3 may also explain the higher affinity of sea bream TTR for T3 than T4. The crystal structure of human TTR in complex with 3,3'-T2 (PDB code: 1THA) reveals that due to more flexible character, 3,3'-T2 moves 3.5 Å deeper (compared to T4) into the central channel and exhibits a twisted conformation of the phenolic and tyrosyl rings.⁴⁶ In contrast, T4 binds to human TTR in skewed conformation. 3'-iodine of 3,3'-T2 also forms I...O XBs with the backbone carbonyl and side chain hydroxyl groups of S117, although the XB formed with side chain hydroxyl ($d_{I...O}$: 2.9 Å, Θ_1 : 102.5°, Θ_2 : 128.7°) is much stronger than with the backbone carbonyl ($d_{I...O}$: 3.2 Å, Θ_1 : 144.8°, Θ_2 : 84.2°). Similar type of interaction is also present in site I; however, only backbone carbonyl of S117 interacts with the 3'-iodine of 3,3'-T2.⁴⁶

In addition to deiodination, THs undergoes a number of metabolic pathways, such as sulphate conjugation, glucuronidation, decarboxylation, and oxidative deamination that lead to the formation of iodothyronine sulphate, glucuronidated iodothyronine, iodothyroamine, and iodothyroacetic acid, respectively.^{35, 51} It is known that iodothyroacetic acid can bind to thyroid hormone receptors (discussed later) and exhibits thyromimetic activity by suppressing TSH levels.⁵² 3,5,3',5'-tetraiodothyroacetic acid (TA4 or tetrac) and 3,5,3'-triiodothyroacetic acid (TA3 or triac) are biosynthesized from T4 and T3, respectively. T4 undergoes oxidative deamination by transaminase to form 3,5,3',5'-tetraiodothyroacetic acid followed by decarboxylation by L-amino acid oxidase (LAO) to form TA4 (Fig. 4a).^{35, 51, 53} TA4 has been shown to be a substrate of iodothyronine deiodinase type I (DIO1) that catalyses the regioselective 5'-deiodination of TA4 to produce TA3 (Fig. 4a).^{35, 51, 54, 55}

Interestingly, TA4 exhibits 2.8-fold higher affinity to human TTR than T4. In contrast to T4, TA4 can bind TTR both in the forward mode and reverse mode. However, the population of reverse binding mode is more in both

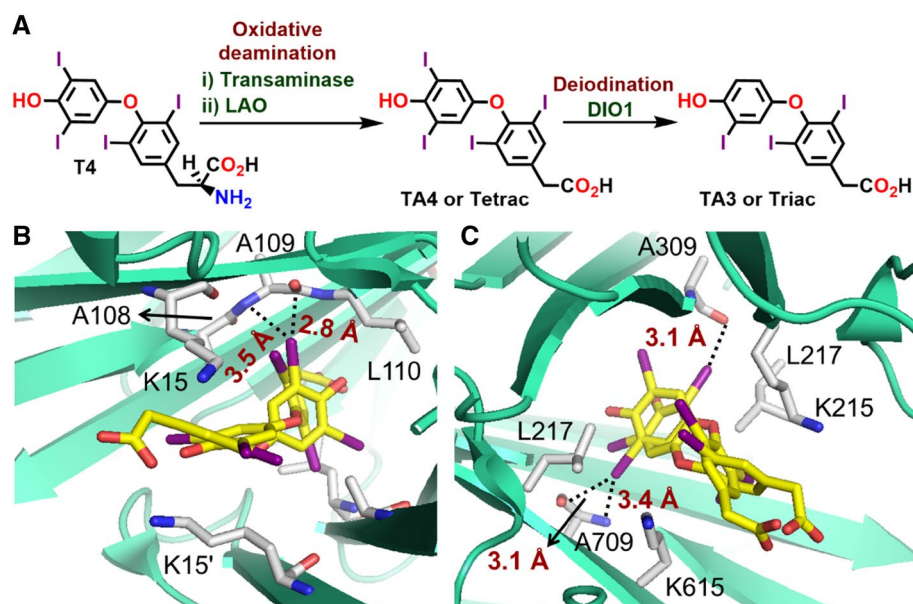


Figure 4: a Biosynthesis of tetraiodothyroacetic acid (TA4) from T4 and deiodination of TA4 by DIO1 to form 3,5,3'-triiodothyroacetic acid (TA3). Crystal structure of human (b, PDB code: 1Z7J)⁵⁶ and rat (c, PDB code: 1KGI)⁵⁷ TTR in complex with TA4, indicating the XB interactions.

the binding sites. The preferable binding in reverse mode may arise due to the small side chain that can penetrate more through the narrow central channel of TTR. Crystal structure of human TTR-TA4 complex (PDB code: 1Z7J) reveals that in the forward mode, the 3'- and 5'-iodine atoms occupy the HBP3 and HBP2' pockets in both the binding sites.⁵⁶ While 4'-OH group does not form hydrogen bond with S117, the carboxylate side chain forms salt-bridge interaction with K15. In the reverse binding mode, 4'-OH group forms hydrogen bond with K15 and the carboxylate side chain occupies the HBP3 pocket. In this mode, the 3- and 5-iodine atoms occupy the HBP1(1') pockets, whereas the 3'- and 5'-iodine atoms occupy HBP2(2') pockets. In both the sites, XB interactions are formed by the 3'-iodine specifically in the forward binding mode (Fig. 4b). For example, 3'-iodine forms a strong I...O XB with the backbone carbonyl of A109 (in site I) and A309 (in site II), although the XB in site I ($d_{I...O}$: 2.8 Å, 20% shorter than the sum of van der Waal's radii) is stronger than in site II ($d_{I...O}$: 3 Å, 14.3% shorter than the sum of van der Waal's radii) (Table 1).⁵⁶ In both the sites, the 3'-iodine also forms I...N XB with the backbone NH of A109 (in site I) and L310 (in site II), and in contrast to I...O XBs, these interactions are of equal strength. Rat TTR also binds TA4 both in the forward and reverse

binding mode in site I, whereas in site II, only forward mode is observed (PDB code: 1KGI).⁵⁷ Similar to human TTR-T4 (monoclinic form) and rat TTR-T4 complexes, 3'- and 5'-iodine atoms in TA4 occupy the HBP3(3') pockets in the forward mode. Two electron densities for TA4 are found in site II and 3'-iodine in both the molecules form two almost identical I...O XBs with the backbone carbonyls of A309 and A709 residues (Fig. 4c and Table 1). Backbone NH of A709 also forms an I...N XB with the 3'-iodine of one of the molecules.⁵⁷ Comparisons of the strength of these XBs with those observed in human TTR-TA4 complex indicate that human TTR may exhibit higher affinity to TA4 than rat TTR.

5 Human Serum Albumin (HSA)

Human Serum Albumin (HSA) is the most abundant protein in human plasma with a molecular weight of 66,437 Da. HSA is mainly responsible for the transport of non-esterified fatty acids, bilirubin, bile acids, steroid, and thyroid hormones. Amongst all three transport proteins, HSA exhibits lowest affinity to T4 ($K_d \sim 2 \mu\text{M}$).^{35, 36} Monomeric HSA contains three homologous domains (I, II and III) and each of these domains contains two subdomains (A and B). Crystal structure of HSA in complex with T4 (PDB code: 1HK1) indicates that there are four T4-binding sites (Tr1, Tr2, Tr3 and Tr4)

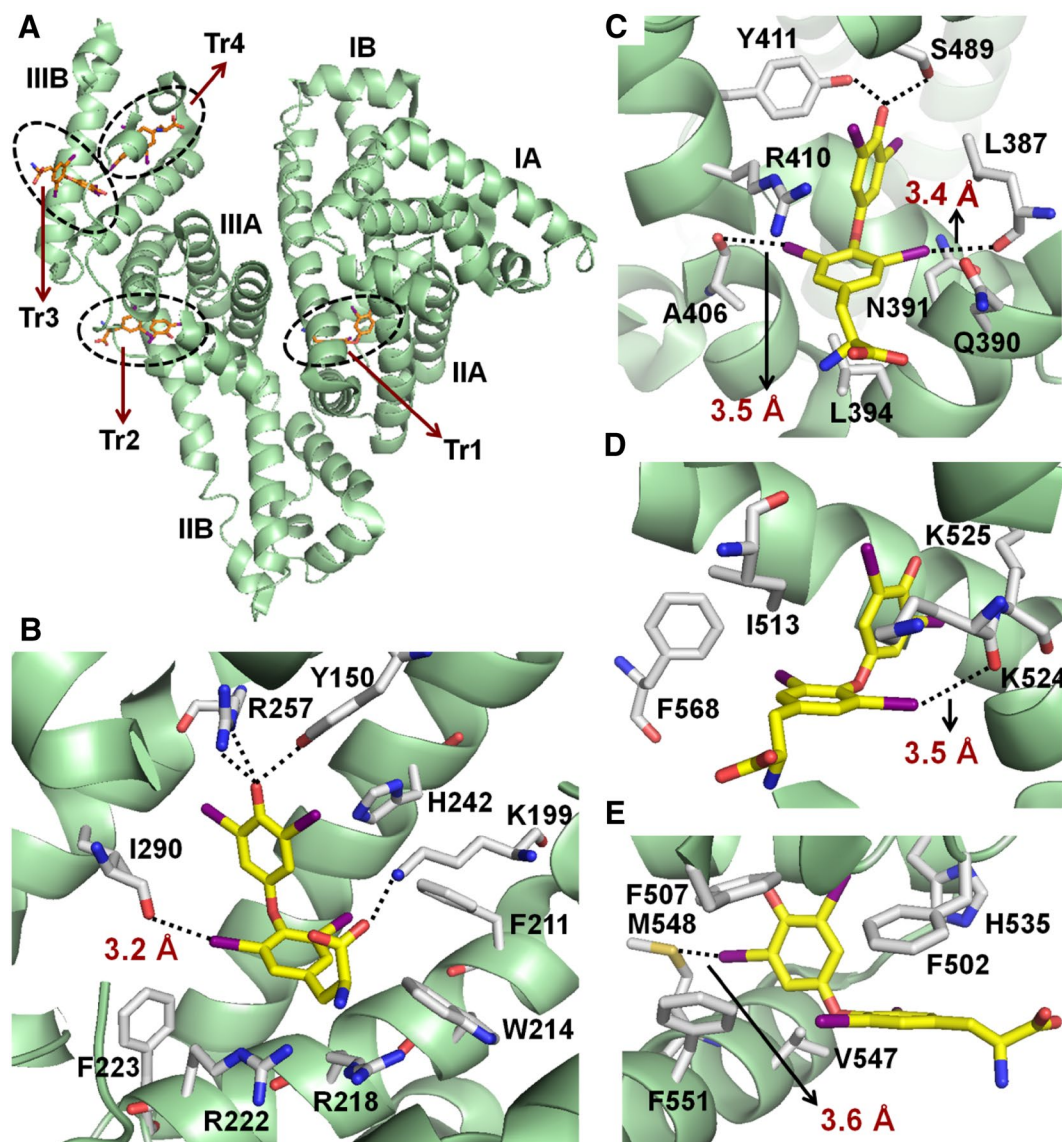
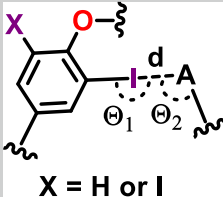


Figure 5: a Thyroxine-binding sites (Tr1, Tr2, Tr3, and Tr4) in human serum albumin (HSA) (PDB code: 1HK1).⁵⁹ Hydrogen bonding and XB interactions between T4 and HSA observed in Tr1 (b), Tr2 (c), Tr3 (d), and Tr4 (e) sites.

in HSA (Fig. 5a).⁵⁸ While Tr1 and Tr2 is located in the subdomains IIA and IIIA, respectively, both Tr3 and Tr4 are located in the IIIB subdomain. Among these four sites, Tr1 exhibits the highest affinity to T4, which exhibits a less stable *cisoid* (the phenolic ring and β -alanine side chain remain in the same faces of the tyrosyl ring) conformation at Tr1, whereas it exhibits the common *transoid* (the phenolic ring and β -alanine side chain remain in the opposite faces of the tyrosyl ring) conformation in the other binding sites.^{59, 60} This is mainly because of the presence of large hydrophobic side chains of F223, R222, R218, and W214 in Tr1, and

these residues push the β -alanine side chain of T4 to the other side of the tyrosyl ring (Fig. 5b). Mainly hydrophobic interactions are responsible for the bonding of T4 to Tr1, although a few hydrogen bonds, such as between 4'-OH group and R257 as well as Y150, carboxylate functionality, and K199 are also observed. The 3-iodine of T4 forms a I...O XB ($d_{I...O}$: 3.2 Å, Θ_1 : 146.6°, Θ_2 : 126.7°) with the backbone carbonyl of I290 (Fig. 5b and Table 2).⁵⁸ Notably, unlike in TTR, the 3'- and 5'-iodine atoms do not form any XBs with HSA. As R218 sterically hinders the β -alanine side chain of T4 in Tr1, mutation of this residue to either His or Pro increases

Table 2: XBs observed in the crystal structures of HSA in complex with T4.


PDB Code	Serum albumin	Ligand (iodine)	XB acceptor (A)	d (Å)	Θ ₁ (°)	Θ ₂ (°)
1HK1	Human	T4 (3)	I290 (backbone O, Tr1)	3.2	146.6	126.7
		T4 (3)	A406 (backbone O, Tr2)	3.5	164.0	92.9
		T4 (5)	L387 (backbone O, Tr2)	3.4	169.9	131.4
		T4 (5)	K524 (backbone O, Tr3)	3.5	151.0	102.3
		T4 (5')	M548 (side chain S, Tr4)	3.6	152.5	110.0
1HK2	Human	T4 (3)	I290 (backbone O, Tr1)	3.3	152.7	129.6
		T4 (3)	A406 (backbone O, Tr2)	3.3	162.1	129.9
		T4 (5)	K524 (backbone O, Tr3)	3.2	143.9	113.7
		T4 (5')	M548 (side chain S, Tr4)	3.6	147.3	118.8
1HK3	Human	T4 (3)	I290 (backbone O, Tr1)	3.4	153.7	133.5
		T4 (3)	A406 (backbone O, Tr2)	3.5	163.0	92.5
		T4 (5)	L387 (backbone O, Tr2)	3.5	169.3	127.4
		T4 (5)	K524 (backbone O, Tr3)	3.1	143.2	119.8
1HK4	Human	T4 (3)	N429 (backbone O, Tr5)	3.2	132.5	113.6
1HK5	Human	T4 (3)	N429 (backbone O, Tr5)	3.5	132.5	111.1

the binding affinity by making more room for the β -alanine side chain of T4. The relaxation of the β -alanine side chain leads to the formation of weaker XB with I290 in the R218H ($d_{I...O}$: 3.3 Å, PDB code 1HK2) and R218P ($d_{I...O}$: 3.4 Å, PDB code 1HK3) mutants (Table 2). However, decrease in XB strength does not lead to a decrease in affinity; rather, R218H and R218P mutants exhibit 10–15-fold higher affinity for T4.⁵⁸ Probably, the other hydrophobic and hydrogen-bonding interactions compensate for the weaker XB.

While in other binding sites (Tr2, Tr3, and Tr4), T4 forms predominantly hydrophobic interactions, two hydrogen-bonding interactions involving the 4'-hydroxyl group of T4 and Y411 and S489 residues are observed in Tr2 (Fig. 5c). Furthermore, in Tr2, the 3- and 5-iodine atoms of T4 make I...O interactions with the backbone carbonyl of A406 ($d_{I...O}$: 3.5 Å) and L387 ($d_{I...O}$: 3.5 Å) residues, respectively (Fig. 5c and Table 2). While the I...O contact with A406 in the wild-type protein is just equal to the sum of van der Waal's radii of iodine and oxygen, it is found to be stronger in R218H mutant ($d_{I...O}$: 3.3 Å, Table 2).⁵⁸ However, in the R218P mutant,

both these interactions with A406 and L387 are really weak ($d_{I...O}$: 3.5 Å). Similarly, in Tr3, the 5-iodine atom forms a weak interaction with backbone carbonyl of K524 of the wild-type protein with I...O distance of 3.5 Å (Fig. 5d). These interactions are much stronger in the R218H ($d_{I...O}$: 3.2 Å) and R218P ($d_{I...O}$: 3.1 Å) mutants (Table 2). In Tr4 of wild-type HSA and R218H mutant, the 5'-iodine of T4 forms I...S XB with the side chain of M548 residue (Fig. 5e and Table 2). These interactions have $d_{I...S}$ of 3.6 Å that is 7.4% shorter than the sum of van der Waals radii of sulphur and iodine (3.78 Å). Also, these interactions have nearly identical Θ_1 and Θ_2 .⁵⁸ However, this I...S XB is absent in the R218P mutant. Altogether, Tr1 forms maximum number of interactions (both hydrogen bonding and XB) and the strongest XB with T4, and these lead to the higher affinity of Tr1 to T4. Interestingly, a new T4-binding site (Tr5) is found between the domains I and III of HSA–myristate complex that binds only one equivalent of T4. In this site, both 4'-hydroxyl group and β -alanine side chain of T4 are solvent exposed, and the other parts of T4 are stabilized by hydrophobic

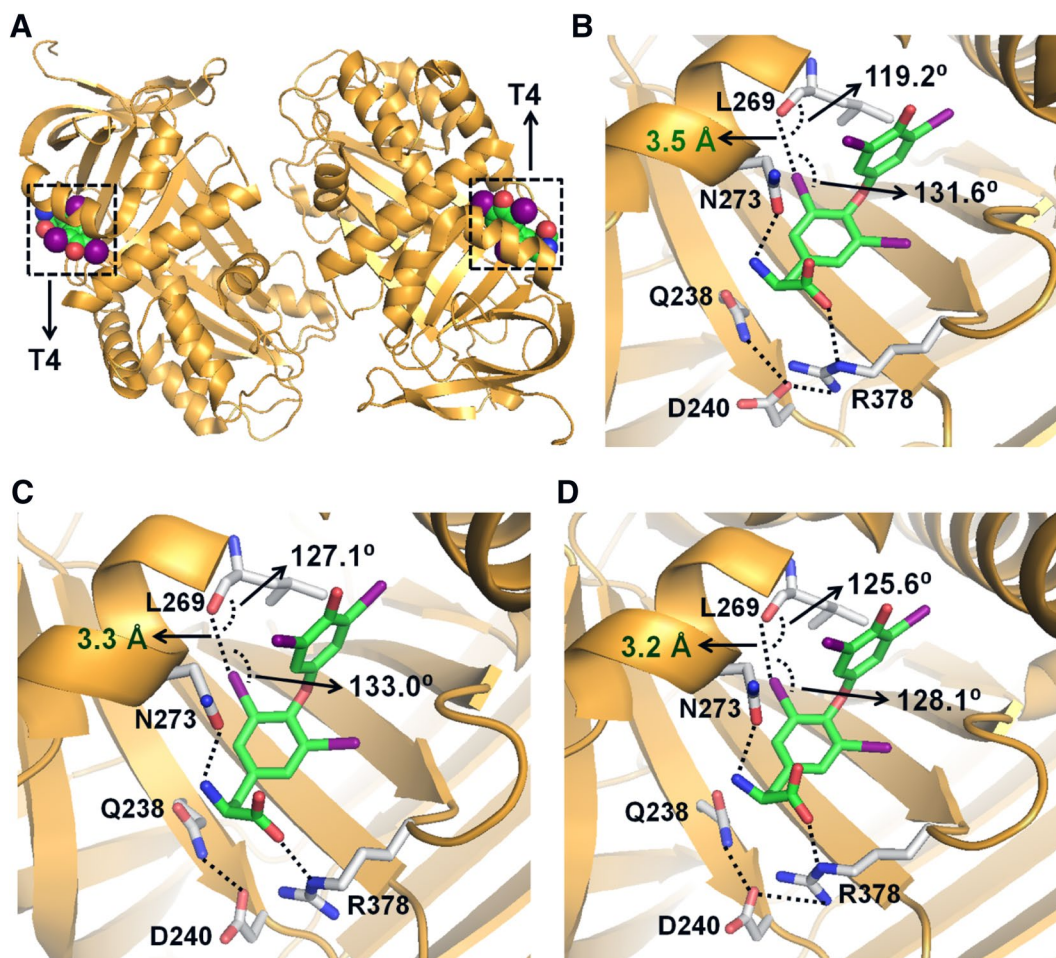


Figure 6: **a** Crystal structure of TBG in complex with T4, indicating the T4-binding sites (PDB code: 2CEO).⁶¹ **b** Hydrogen bonding and XB interactions between T4 and TBG observed in human TBG (PDB code: 2CEO) and human TBG without the reactive centre loop (**c**, PDB code: 2RIW).^{61, 62} **d** Hydrogen bonding and XB interactions observed in the cocystal of human TBG and T4-fluorescein conjugate (PDB code: 2XN6).⁶² Fluorescein part is not shown for clarity.

interactions. One prominent I...O XB is formed between the backbone carbonyl of N429 and 3-iodine atom of T4 with $d_{I...O}$ of 3.2 Å (Table 2). However, in R218H mutant, this interaction is not prominent ($d_{I...O}$: 3.5 Å).⁵⁸

6 Thyroxine-binding globulin (TBG)

Thyroxine-binding globulin (TBG), the principal thyroxine carrier in serum, is a member of serine protease inhibitor (SERPIN) family. It has the highest affinity to T4 with a K_d value of 0.1 nM.^{35, 36} TBG contains two identical sites for T4 in a surface cavity between helices H and A, and strands 3–5 of the β -sheet (Fig. 6a).⁶¹ T4 at these sites mainly forms a series of hydrophobic interactions. Also the β -alanine side chain forms hydrogen-bonding interactions with N273 and

R378 residues (Fig. 6b). Furthermore, 3-iodine of T4 forms a weak I...O interaction ($d_{I...O}$: 3.5 Å, Θ_1 : 131.6°, Θ_2 : 119.2°) with the backbone carbonyl of L269.⁶¹ Unlike other transporter proteins, T4 release from TBG is controlled by an allosteric mechanism.^{61, 62} Similar to other protease inhibitors in SERPIN family, TBG contains a reactive centre loop (RCL), and the cleavage of this loop leads to an irreversible change in the conformation of TBG. This conformational change leads to an almost threefold decrease in the affinity to T4. The crystal structure of human TBG with cleaved RCL in complex with T4 reveals that the β -alanine side chain of T4 forms the hydrogen-bonding interactions with N273 and R378 residues, similar to the uncleaved protein (Fig. 6b, c, PDB code: 2RIW).⁶² It is observed that the 3-iodine atom forms a stronger I...O XB

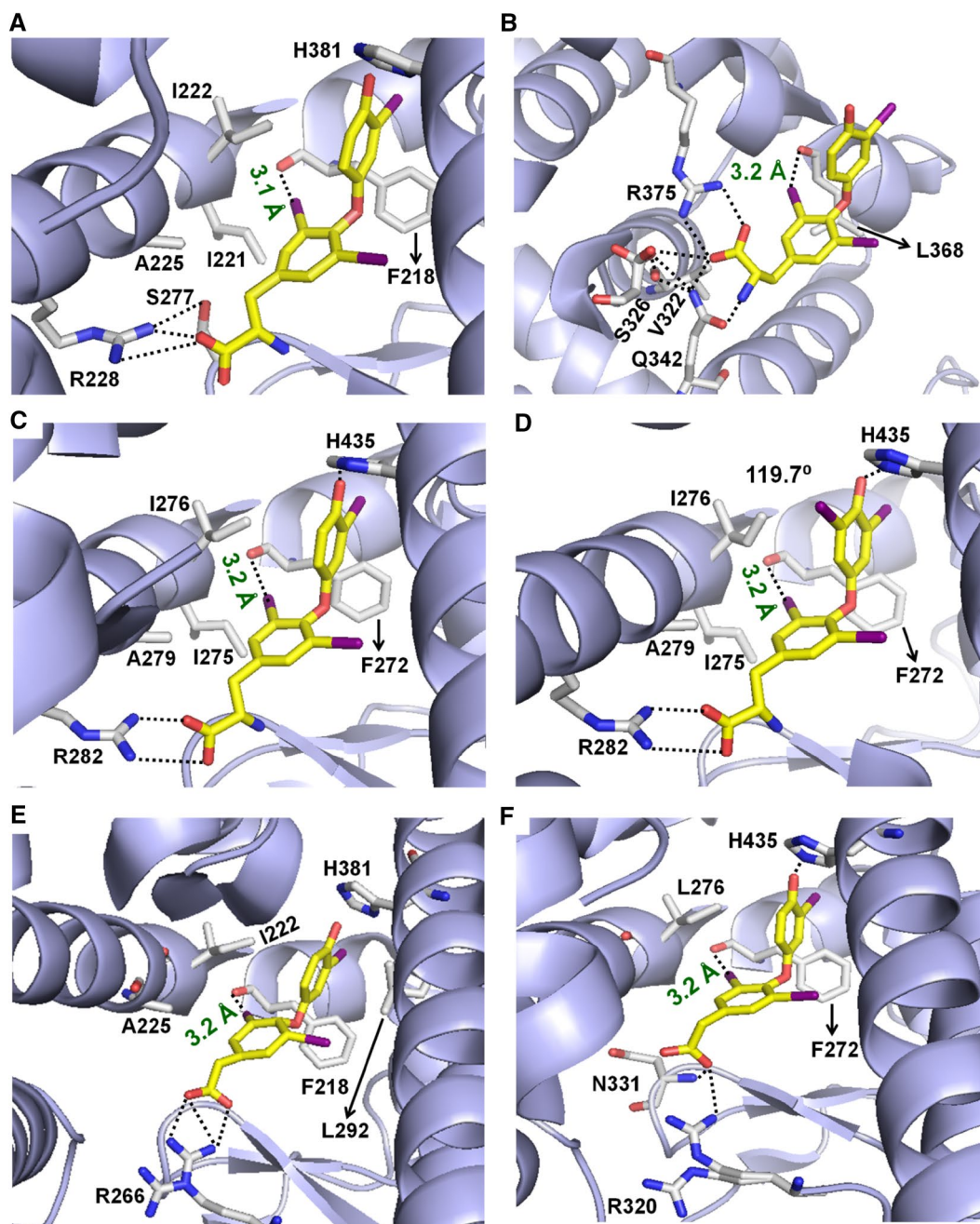
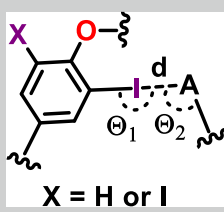


Figure 7: **a, b** Hydrogen bonding and XBs observed in the T3-binding sites of Tr α 1 (PDB codes: 2H77 and 4LNW).^{67, 68} Crystal structures of TR β in complex with T3 (**c**, PDB code: 1XZX) and T4 (**d**, PDB code: 1Y0X).⁶⁹ Crystal structures of TR α (**e**, PDB code: 3JZB) and TR β (**f**, 3JZC) in complex with triiodothyroacetic acid (TA3).⁷⁰

with L269 residue than the uncleaved protein. This XB has $d_{1...O}$ of 3.3 Å, and Θ_1 and Θ_2 are almost similar to that observed in the uncleaved protein complex (Fig. 6b, c). Human TBG has also been crystallized with a T4-fluorescein conjugate and this conjugate forms the strongest I...O XB among the three described above ($d_{1...O}$:

3.2 Å, Θ_1 : 128.1°, Θ_2 : 125.6°) with the backbone carbonyl of L269 residue (Fig. 6d).⁶² These results indicate that in addition to hydrogen bonding and hydrophobic interactions, XB also play an important role in the molecular recognition of T4 by TBG.

Table 3: XBs observed in the crystal structures of TRs in complex with THs and their metabolites.


PDB Code	Receptor	Ligand (iodine)	XB acceptor (A)	d (Å)	Θ_1 (°)	Θ_2 (°)
2H77	TR α 1 (monoclinic)	T3 (3)	F218 (backbone O)	3.1	174.4	113.6
2H79	TR α 1 (orthorhombic)	T3 (3)	F218 (backbone O)	3.1	173.3	121.2
4LNW	TR α 1	T3 (3)	L368 (backbone O)	3.2	154.8	121.5
4LNX	TR α 1	T4 (3)	L368 (backbone O)	3.2	164.6	121.3
1XZX	TR β	T3 (3)	F272 (backbone O)	3.2	165.9	121.8
1Y0X	TR β	T4 (3)	F272 (backbone O)	3.2	167.6	119.7
3JZB	TR α	T3A	F218 (backbone O)	3.2	169.6	123.4
3JZC	TR β	T3A	F272 (backbone O)	3.2	173.5	119.7

7 Thyroid hormone receptors (TRs)

Thyroid hormone receptors (TRs) are members of nuclear receptors superfamily that regulate gene transcription and translation upon binding to the biologically active TH, T3. The binding of T3 induces a conformational change of the receptor that helps in binding the co-regulator proteins. Furthermore, TRs bind the promoter region of the target gene by recognizing specific nucleotide sequences, called as thyroid hormone response elements (TRES).^{42, 63, 64} There are two genes of TRs (THRA and THRB) and differential splicing of these genes lead to the production of four different receptor isoforms designated as TR α 1, TR α 2, TR β 1, and TR β 2. Expression of these isoforms are tissue-specific—TR α 1 has highest expression in heart and skeletal muscle; TR β 1 is expressed in liver, kidney, and brain; TR β 2 is expressed in anterior pituitary and hypothalamus. While TR α 1 is involved in the maintenance of cardiovascular functions, TR β 1 is mainly associated with metabolism of cholesterol and lipoproteins.^{42, 65, 66} Similar to other nuclear receptors, TRs also have four domains—N terminal A/B domain (NTD), DNA-binding domain (DBD), C-terminal ligand-binding domain (LBD), and a small hinge between LBD and DBD.⁴² The ligand-binding pocket of both subtypes of TRs differs only by a single amino acid residue (S277 in TR α and N331 in TR β).^{35, 52} Both the receptor subtypes have almost 30-fold

higher affinity for T3 ($K_d=0.06$ nM) over T4 ($K_d=2$ nM). The X-ray crystal structure of TR α 1 in complex with T3 (monoclinic form, PDB code: 2H77) reveals that T3 binds inside a hydrophobic core of LBD, and the ligand-binding pocket is made up with several residues from helix 5–6 (H5–6, Met256–Arg266), helix 7–8 (H7–8), and the intervening loop (Leu287–Ile299), helix3 (H3, Phe215–Arg228), helix 11 (H11, His381–His387), and helix 12 (H12, Phe401–Phe405).⁶⁷ TR α 1-bound T3 exhibits the more stable *transoid* conformation and forms mainly hydrophobic interactions, although the carboxylate group is involved in hydrogen bonding with R228 (Fig. 7a). Interestingly, the 3-iodine atom forms a I...O XB with backbone carbonyl of F218 with $d_{I...O}$ of 3.1 Å, which is 11.4% than the sum of the van der Waal's radii of oxygen and iodine. The Θ_1 (174.4°) and Θ_2 (113.6°) of this XB also match the ideal geometry proposed for XB formation (Table 3). Similar XB is also found in the orthorhombic form of TR α 1 in complex with T3 (Table 3, PDB code: 2H79).⁶⁷

Recently Souza et al. have shown that T3 can bind to a separate site located between helix H9, H10, and H11 on the surface of TR α 1.⁶⁸ This binding affinity at this new site is of the order of plasma or intracellular concentration of T3 and T4, indicating that THs can bind to this under physiological conditions. Crystal structure of TR α 1 bound to T3 at this new (noncanonical)

site (PDB code: 4LNW) reveals that T3 exhibits *cisoid* conformation unlike in the canonical site in LBD. T3 binds to this site mainly by hydrogen-bonding interactions with Q342, S326 and R375 residues (Fig. 7b). Furthermore, the backbone carbonyl of L368 forms an XB interaction with the 3-iodine of T3 with $d_{I...O}$: 3.2 Å, Θ_1 : 154.8°, and Θ_2 : 121.5° (Table 3).⁶⁸ T4 can also bind to this site, and exhibits similar conformation and interactions with TR α 1 (PDB code: 4LNX). Notably, similar to T3, the 3-iodine of T4 also forms an I...O XB with L368 (Table 3).⁶⁸

The crystal structure of TR β in complex with T3 (PDB code: 1XZX) indicates that T3 exhibit similar binding interactions as observed in the TR α 1-T3 complex.⁶⁹ While the carboxylate group of T3 interacts with S277 in TR α 1, it forms hydrogen bond with R282 and N331 in TR β (Fig. 7c). Furthermore, unlike in TR α 1, the 4'-hydroxyl group forms hydrogen bond with H435 in TR β . In the hydrophobic core, the 3-iodine of T3 forms XB with backbone carbonyl of F272 with $d_{I...O}$ of 3.2 Å, which is 8.6% shorter than the sum of van der Waal's radii of iodine and oxygen (Table 3). The Θ_1 (165.9°) and Θ_2 (121.8°) of this XB are very similar to those observed in the TR α 1-T3 complex (Table 3).⁶⁹ T4 exhibits lower affinity than T3 due to the presence of two bulky phenolic ring iodine atoms that create strong steric hindrance in ligand-binding pocket. The crystal structure of TR β in complex with T4 (PDB code: 1Y0X) reveals that T4 binding leads to an expansion of the ligand-binding pocket to accommodate the bulky 5'-iodine. Like T3, the 3-iodine atom of T4 forms a XB with backbone carbonyl of F272 with $d_{I...O}$: 3.2 Å, Θ_1 : 167.6°, and Θ_2 : 119.7°.⁶⁹ Although T4 forms identical interactions with TR β as T3, the lower affinity of T4 may result from the deformation of the ligand-binding pocket to accommodate the bulky 5'-iodine.

As mentioned earlier, 3,5,3'-triiodothyroacetic acid (TA3) exhibits thymimetic activity by binding to TRs.^{35, 52} Interestingly, TA3 is found to be threefold more selective to TR β than TR α , indicating that triac can be used for treating thyroid hormone resistance syndrome (RTH) that results from the mutations in TR β 1 gene. Comparison of the crystal structures of TR α -TA3 (PDB code: 3JZB) and TR β -TA3 (PDB code: 3JZC) complexes reveal that TA3 forms hydrogen bond with R266 in TR α , whereas it forms hydrogen bonds with H435, N331, and R320 in TR β (Figs. 7e, f).⁷⁰ In the hydrophobic core, the 3-iodine of TA3 makes moderately strong I...O

XBs with F218 (in TR α) and F272 (in TR β). Both of these XBs are found to be of equal strength and to have almost identical Θ_1 and Θ_2 (Table 3). The TR β selectivity of TA3 is explained on the basis of higher volume of ligand-bonding pocket (500 Å³ in TR β versus 461 Å³ in TR α) in TR β that allows more solvation and flexibility of the acetic acid side chain of TA3.⁷⁰

8 Conclusions

In this minireview, we have discussed the molecular interactions that are responsible for the binding of thyroid hormones and their metabolites with various serum transport proteins and thyroid hormone receptors with a special emphasis on the halogen bonds (XBs). All the serum transport proteins for thyroxine form XBs with T4 as well as the deiodinated metabolites, T3. While transthyretin extensively forms XBs with the phenolic ring iodine atoms of T4 and T3, thyroxine-binding globulin forms XB only with tyrosyl ring iodine of T4. However, human serum albumin can form XBs with both phenolic and tyrosyl ring iodine in different binding sites. Furthermore, in addition to hydrogen bonding, XBs also play important roles in the binding of T4 and T3 to the thyroid hormone receptors (TRs), TR α and TR β . Similar to TBG, TRs also form XBs with only tyrosyl ring iodine. Triiodothyroacetic acid, an endogenous TH metabolite, that exhibits thymimetic activity also forms XBs with TRs. Although the backbone carbonyl and amide groups are predominant, side chain hydroxyl of Ser, and sulphur atom of Met also function as XB acceptors in a few XBs. The presence of such interactions with thyroxine and its metabolites indicates that the biological systems use iodine atoms as part of the thyroid hormones to provide higher selectivity of these key hormones to the transport proteins and receptors.

Publisher's Note

Springer Nature remains neutral with regard to jurisdictional claims in published maps and institutional affiliations.

Received: 16 November 2019 Accepted: 11 December 2019

Published online: 23 December 2019

References

1. Metrangolo P, Resnati G (2013) Metal-bound halogen atoms in crystal engineering. *Chem Commun* 49:1783–1785

- Nakamoto K, Margoshes M, Rundle RE (1955) Stretching frequencies as a function of distances in hydrogen bonds. *J Am Chem Soc* 77:6480–6486
- Von P, Schleyer R, West R (1959) Comparison of covalently bonded electro-negative atoms as proton acceptor groups in hydrogen bonding. *J Am Chem Soc* 81:3164–3165
- Colin M (1814) Note Sur Quelques Combinaisons de L'iode. *Ann Chim* 91:252–272
- Pelletier JCP (1819) Sur Un Nouvel Alkali Végétal (la Strychine) Trouvé Dans La Fève de Saint-Ignace, La Noix Vomique Etc., *Ann Chim Phys* 10:142–177
- P. N. 2009-032-1-100 (2010) Categorizing halogen bonding and other noncovalent interactions involving halogen atoms. *Chem Int* 32:20–21
- Desiraju GRH, Ho PS, Kloos L, Legon AC, Marquardt R, Metrangolo P, Politzer P, Resnati G, Rissanen K (2013) Definition of the halogen bond (IUPAC Recommendations 2013). *Pure Appl Chem* 85:1711–1713
- Clark T, Hennemann M, Murray JS, Politzer P (2007) Halogen bonding: the sigma-hole. In: Proceedings of “Modeling interactions in biomolecules II”, Prague, 5th–9th September 2005, *J Mol Model* 13:291–296
- Murray JS, Lane P, Clark T, Politzer P (2007) Sigma-hole bonding: molecules containing group VI atoms. *J Mol Model* 13:1033–1038
- Auffinger P, Hays FA, Westhof E, Ho PS (2004) Halogen bonds in biological molecules. *Proc Natl Acad Sci USA* 101:16789–16794
- Valerio G, Raos G, Meille SV, Metrangolo P, Resnati G (2000) Halogen bonding in fluoroalkylhalides: a quantum chemical study of increasing fluorine substitution. *J Phys Chem A* 104:1617–1620
- Gao K, Goroff NS (2000) Two New iodine-capped carbon rods. *J Am Chem Soc* 122:9320–9321
- Sun A, Lauher JW, Goroff NS (2006) Preparation of poly(diododiacetylene), an ordered conjugated polymer of carbon and iodine. *Science* 312:1030–1034
- Zou JW, Jiang YJ, Guo M, Hu GX, Zhang B, Liu HC, Yu QS (2005) Ab initio study of the complexes of halogen-containing molecules RX (X = Cl, Br, and I) and NH₃: towards understanding the nature of halogen bonding and the electron-accepting propensities of covalently bonded halogen atoms. *Chem Eur J* 11:740–751
- Ananthavel SP, Manoharan M (2001) A theoretical study on electron donor–acceptor complexes of Et₂O, Et₂S and Me₃N with interhalogens, I-X (X = Cl and Br). *Chem Phys* 269:49–57
- Cavallo G, Metrangolo P, Milani R, Pilati T, Priimagi A, Resnati G, Terraneo G (2016) The halogen bond. *Chem Rev* 116:2478–2601
- Gilday LC, Robinson SW, Barendt TA, Langton MJ, Mullaney BR, Beer PD (2015) Halogen bonding in supramolecular chemistry. *Chem Rev* 115:7118–7195
- Metrangolo P, Meyer F, Pilati T, Resnati G, Terraneo G (2008) Halogen bonding in supramolecular chemistry. *Angew Chem Int Ed* 47:6114–6127
- Metrangolo P, Neukirch H, Pilati T, Resnati G (2005) Halogen bonding based recognition processes: a world parallel to hydrogen bonding. *Acc Chem Res* 38:386–395
- Ford MC, Ho PS (2016) Computational tools to model halogen bonds in medicinal chemistry. *J Med Chem* 59:1655–1670
- Hays FA, Teegarden A, Jones ZJ, Harms M, Raup D, Watson J, Cavaliere E, Ho PS (2005) How sequence defines structure: a crystallographic map of DNA structure and conformation. *Proc Natl Acad Sci USA* 102:7157–7162
- Hays FA, Vargason JM, Ho PS (2003) Effect of sequence on the conformation of DNA holliday junctions. *Biochemistry* 42:9586–9597
- Mendez L, Henriquez G, Sirimulla S, Narayan M (2017) Looking back, looking forward at halogen bonding in drug discovery. *Molecules* 22:1397
- Parisini E, Metrangolo P, Pilati T, Resnati G, Terraneo G (2011) Halogen bonding in halocarbon-protein complexes: a structural survey. *Chem Soc Rev* 40:2267–2278
- Wilcken R, Zimmermann MO, Lange A, Joerger AC, Boeckler FM (2013) Principles and applications of halogen bonding in medicinal chemistry and chemical biology. *J Med Chem* 56:1363–1388
- Mondal S, Gong X, Zhang X, Salinger AJ, Zheng L, Sen S, Weerapana E, Thompson PR (2019) Halogen bonding increases the potency and isozyme selectivity of protein arginine deiminase 1 Inhibitors. *Angew Chem Int Ed* 58:12476–12480
- Jakka SR, Govindaraj V, Mugesh G (2019) A Single Atom Change Facilitates the Membrane Transport of Green Fluorescent Proteins in Mammalian Cells. *Angew Chem Int Ed* 58:7713–7717
- Ungati H, Govindaraj V, Mugesh G (2018) The remarkable effect of halogen substitution on the membrane transport of fluorescent molecules in living cells. *Angew Chem Int Ed* 57:8989–8993
- Ungati H, Govindaraj V, Nair CR, Mugesh G (2019) Halogen-mediated membrane transport: an efficient strategy for the enhancement of cellular uptake of synthetic molecules. *Chem Eur J* 25:3391–3399
- Lu Y, Wang Y, Zhu W (2010) Nonbonding interactions of organic halogens in biological systems: implications for drug discovery and biomolecular design. *Phys Chem Chem Phys* 12:4543–4551
- Brent GA (2012) Mechanisms of thyroid hormone action. *J Clin Invest* 122:3035–3043
- Fekete C, Lechan RM (2007) Negative feedback regulation of hypophysiotropic thyrotropin-releasing hormone (TRH) synthesizing neurons: role of neuronal afferents and type 2 deiodinase. *Front Neuroendocrinol* 28:97–114
- Lechan RM, Fekete C (2004) Feedback regulation of thyrotropin-releasing hormone (TRH): mechanisms for the non-thyroidal illness syndrome. *J Endocrinol Invest* 27:105–119

34. Mullur R, Liu YY, Brent GA (2014) Thyroid hormone regulation of metabolism. *Physiol Rev* 94:355–382
35. Mondal S, Raja K, Schweizer U, Mugesh G (2016) Chemistry and biology in the biosynthesis and action of thyroid hormones. *Angew Chem Int Ed* 55:7606–7630
36. Schussler GC (2000) The thyroxine-binding proteins. *Thyroid* 10:141–149
37. Berry MJ, Banu L, Larsen PR (1991) Type I iodothyronine deiodinase is a selenocysteine-containing enzyme. *Nature* 349:438–440
38. Bianco AC, Salvatore D, Gereben B, Berry MJ, Larsen PR (2002) Biochemistry, cellular and molecular biology, and physiological roles of the iodothyronine selenodeiodinases. *Endocr Rev* 23:38–89
39. Kohrle J (2002) Iodothyronine deiodinases. *Methods Enzymol* 347:125–167
40. Schweizer U, Steegborn C (2015) New insights into the structure and mechanism of iodothyronine deiodinases. *J Mol Endocrinol* 55:R37–R52
41. Davis PJ, Goglia F, Leonard JL (2016) Nongenomic actions of thyroid hormone. *Nat Rev Endocrinol* 12:111–121
42. Yen PM (2001) Physiological and molecular basis of thyroid hormone action. *Physiol Rev* 81:1097–1142
43. Eisele YS, Monteiro C, Fearn C, Encalada SE, Wiseman RL, Powers ET, Kelly JW (2015) Targeting protein aggregation for the treatment of degenerative diseases. *Nat Rev Drug Discov* 14:759–780
44. Wojtczak AC, Cody V, Luft JR, Pangborn W (1996) Structures of human transthyretin complexed with thyroxine at 2.0 Å resolution and 3',5'-dinitro-*N*-acetyl-L-thyronine at 2.2 Å resolution. *Acta Crystallogr Sect D* 52:758–765
45. Eneqvist T, Lundberg E, Karlsson A, Huang S, Santos CR, Power DM, Sauer-Eriksson AE (2004) High resolution crystal structures of piscine transthyretin reveal different binding modes for triiodothyronine and thyroxine. *J Biol Chem* 279:26411–26416
46. Wojtczak A, Luft J, Cody V (1992) Mechanism of molecular recognition. Structural aspects of 3,3'-diiodo-L-thyronine binding to human serum transthyretin. *J Biol Chem* 267:353–357
47. Wojtczak AN, Neumann P, Cody V (2001) Structure of a new polymorphic monoclinic form of human transthyretin at 3 Å resolution reveals a mixed complex between unliganded and T4-bound tetramers of TTR. *Acta Crystallogr Sect D* 57:957–967
48. Hamilton JA, Steinrauf LK, Braden BC, Liepnieks J, Benson MD, Holmgren G, Sandgren O, Steen L (1993) The X-ray crystal structure refinements of normal human transthyretin and the amyloidogenic Val-30->Met variant to 1.7-Å resolution. *J Biol Chem* 268:2416–2424
49. Steinrauf LK, Hamilton JA, Braden BC, Murrell JR, Benson MD (1993) X-ray crystal structure of the Ala-109->Thr variant of human transthyretin which produces euthyroid hyperthyroxinemia. *J Biol Chem* 268:2425–2430
50. Wojtczak AC, Cody V, Luft JR, Pangborn W (2001) Structure of rat transthyretin (rTTR) complex with thyroxine at 2.5 Å resolution: first non-biased insight into thyroxine binding reveals different hormone orientation in two binding sites. *Acta Crystallogr Sect D* 57:1061–1070
51. Wu SY, Green WL, Huang WS, Hays MT, Chopra IJ (2005) Alternate pathways of thyroid hormone metabolism. *Thyroid* 15:943–958
52. Mondal S, Mugesh G (2017) Novel thyroid hormone analogues, enzyme inhibitors and mimetics, and their action. *Mol Cell Endocrinol* 458:91–104
53. Moreno M, De Lange P, Lombardi A, Silvestri E, Lanni A, Goglia F (2008) Metabolic effects of thyroid hormone derivatives. *Thyroid* 18:239–253
54. Koehrle J, Auf'mkolk M, Rokos H, Hesch RD, Cody V (1986) Rat liver iodothyronine monodeiodinase. Evaluation of the iodothyronine ligand-binding site. *J Biol Chem* 261:11613–11622
55. Shepherdley CA, Klootwijk W, Makabe KW, Visser TJ, Kuiper GG (2004) An ascidian homolog of vertebrate iodothyronine deiodinases. *Endocrinology* 145:1255–1268
56. Neumann PC, Cody V, Wojtczak A (2005) Ligand binding at the transthyretin dimer-dimer interface: structure of the transthyretin-T4Ac complex at 2. Å resolution. *Acta Crystallogr Sect D* 61:1313–1319
57. Muziol TC, Cody V, Luft JR, Pangborn W, Wojtczak A (2001) Complex of rat transthyretin with tetraiodothyroacetic acid refined at 2.1 and 1.8 Å resolution. *Acta Biochim Pol* 48:877–884
58. Petitpas I, Petersen CE, Ha CE, Bhattacharya AA, Zunszain PA, Ghuman J, Bhagavan NV, Curry S (2003) Structural basis of albumin–thyroxine interactions and familial dysalbuminemic hyperthyroxinemia. *Proc Natl Acad Sci USA* 100:6440–6445
59. Mondal S, Mugesh G (2015) Structure elucidation and characterization of different thyroxine polymorphs. *Angew Chem Int Ed* 54:10833–10837
60. Mondal S, Mugesh G (2016) Conformational flexibility and halogen bonding in thyroid hormones and their metabolites. *Cryst Growth Des* 16:5896–5906
61. Zhou A, Wei Z, Read RJ, Carrell RW (2006) Structural mechanism for the carriage and release of thyroxine in the blood. *Proc Natl Acad Sci USA* 103:13321–13326
62. Qi X, Loiseau F, Chan WL, Yan Y, Wei Z, Milroy LG, Myers RM, Ley SV, Read RJ, Carrell RW, Zhou A (2011) Allosteric modulation of hormone release from thyroxine and corticosteroid-binding globulins. *J Biol Chem* 286:16163–16173
63. Evans RM (1988) The steroid and thyroid hormone receptor superfamily. *Science* 240:889–895

64. Nagy L, Schwabe JW (2004) Mechanism of the nuclear receptor molecular switch. *Trends Biochem Sci* 29:317–324
65. Gullberg H, Rudling M, Salto C, Forrest D, Angelin B, Vennstrom B (2002) Requirement for thyroid hormone receptor beta in T3 regulation of cholesterol metabolism in mice. *Mol Endocrinol* 16:1767–1777
66. Mittag J, Davis B, Vujovic M, Arner A, Vennstrom B (2010) Adaptations of the autonomous nervous system controlling heart rate are impaired by a mutant thyroid hormone receptor-alpha1. *Endocrinology* 151:2388–2395
67. Nascimento AS, Dias SM, Nunes FM, Aparicio R, Ambrosio AL, Bleicher L, Figueira AC, Santos MA, De Oliveira Neto M, Fischer H, Togashi M, Craievich AF, Garratt RC, Baxter JD, Webb P, Polikarpov I (2006) Structural rearrangements in the thyroid hormone receptor hinge domain and their putative role in the receptor function. *J Mol Biol* 360:586–598
68. Souza PC, Puhl AC, Martinez L, Aparicio R, Nascimento AS, Figueira AC, Nguyen P, Webb P, Skaf MS, Polikarpov I (2014) Identification of a new hormone-binding site on the surface of thyroid hormone receptor. *Mol Endocrinol* 28:534–545
69. Sandler B, Webb P, Apriletti JW, Huber BR, Togashi M, Cunha Lima ST, Juric S, Nilsson S, Wagner R, Fletterick RJ, Baxter JD (2004) Thyroxine-thyroid hormone receptor interactions. *J Biol Chem* 279:55801–55808
70. Martinez L, Nascimento AS, Nunes FM, Phillips K, Aparicio R, Dias SM, Figueira AC, Lin JH, Nguyen P, Apriletti JW, Neves FA, Baxter JD, Webb P, Skaf MS, Polikarpov I (2009) Gaining ligand selectivity in thyroid hormone receptors via entropy. *Proc Natl Acad Sci USA* 106:20717–20722



Santanu Mondal was born in 1988 in West Bengal, India. After finishing B.Sc. from Jadavpur University, Kolkata, he joined Indian Institute of Science, Bangalore from where he received M.S. and Ph.D. in 2011 and 2016, respectively. During

Ph.D., he worked on the biomimetic deiodination of thyroid hormones and metabolites under the supervision of Prof. G. Mugesh. Currently, he is a post-doctoral fellow in the laboratory of Prof. Paul R. Thompson at University of Massachusetts Medical School, USA. His current research interests include development of small molecule inhibitors and chemical probes of protein arginine deiminases (PADs) that are associated with several autoimmune diseases and cancer.



Debasish Giri obtained his B.Sc. from Midnapore college, West Bengal, in 2015 and MS from Indian Institute of Science, Bangalore in 2017. Currently, he is carrying out his Ph.D. research under the guidance of Prof. G. Mugesh. His work is mainly

focussed on the deiodination of thyroxine and thyroxine analogues by synthetic deiodinase mimics.



Govindasamy Mugesh received his Ph.D. degree from the Indian Institute of Technology, Bombay in 1998. After completing his post-doctoral studies, he joined as Assistant Professor in 2002 at the Indian Institute of Science, Bangalore, where he is currently a

Professor. His research interests include chemistry of thyroid hormone metabolism, development of novel therapeutics for endothelial dysfunction and neurodegenerative diseases and nanomaterials for biological applications.